

Copyright © 1965, by the author(s).  
All rights reserved.

Permission to make digital or hard copies of all or part of this work for personal or classroom use is granted without fee provided that copies are not made or distributed for profit or commercial advantage and that copies bear this notice and the full citation on the first page. To copy otherwise, to republish, to post on servers or to redistribute to lists, requires prior specific permission.

Electronics Research Laboratory  
University of California  
Berkeley, California  
Internal Technical Memorandum M-118

ABSOLUTE RADIATION STANDARD IN  
THE FAR INFRARED

by

A. J. Lichtenberg  
S. Sesnic

This work was supported in part by the Joint Services Electronics Program (U.S. Army, U. S. Navy, and U.S. Air Force) under Grant No. AF-AFOSR-139-64; the U.S. Air Force under Contract No. AF33(615)-1078, and the National Science Foundation under Grant No. NSF GP-2239.

May 27, 1965

## ABSTRACT

An absolute radiation standard is constructed for use between 200 and 2000  $\mu$ . It is demonstrated that the output is that of a blackbody over this wavelength range. The absolute standard is used to calibrate a secondary standard mercury arc lamp which is found to have an equivalent temperature in the neighborhood of 3000<sup>o</sup> K. It is shown that absolute standards can be used either to determine the strength of an unknown signal directly or to calibrate the sensitivity of a monochromator-detector system.

## INTRODUCTION

For measurements of emission in the far infrared (200 to 2000  $\mu$ ) it is often desirable to know the absolute intensity of the radiation. Measurements of this nature have become increasingly important in plasma physics both to determine the state of the plasma,<sup>1</sup> and as a check on the theory of plasma radiation.<sup>2</sup> In addition, information obtained from measurements of solar, planetary, and cosmic radiation could be greatly enhanced by using frequencies within this band.<sup>3</sup>

In the near infrared, absolute measurements have been made by using a black radiation detector<sup>4</sup> or a standard blackbody source.<sup>5</sup> Although the use of a black detector is most convenient, knowledge of the transmission characteristics of the spectrometer is then essential. It also becomes increasingly difficult to obtain adequate time response at the longer wavelengths.<sup>5</sup> This is particularly true for observations of transient signals in pulsed plasma devices for which photodetectors are normally used. In principle, a standard blackbody suffers from neither of these difficulties. The response to the desired signal can be compared directly with the response to the standard source, thus obtaining absolute intensity measurements without additional calibration. Also, at least in principle, we can insure that the source is black by using a large enough cavity with a small hole. In practice, there are considerable difficulties in achieving these ends which will be discussed in later sections. A further difficulty is that the radiation intensity from a source at moderate temperature (say 500<sup>o</sup> K) is difficult to detect at the

longer wavelengths. These measurements did, indeed, prove difficult and were only accomplished with a photodetector having peak sensitivity near  $1000 \mu^6$  and radiometric techniques with long integration times.

The basic method of insuring the blackness of a source is to design two blackbodies of very different configurations and theoretical emissivities. Without knowing the absolute emissivity of the surface, one can calculate the difference in the emissivity of the two blackbodies as a function of their absolute emissivities. Measurements of this difference can then be made to determine whether the absolute emissivity is acceptable. The results can then be checked by measuring the surface emissivity of the blackbody material by reflectivity measurements, then verifying that the calculated values of blackbody emissivity lie within the range indirectly measured. The theory and calculation will be presented in the next section.

An important aspect of absolute intensity measurements is the calibration of secondary standards. The intensity of radiation from mercury discharges is known to be much higher than thermal sources within the wavelength range of interest. After the spectral distribution of radiation from such a source has been calibrated against an absolute standard, it can then be used as a secondary standard affording considerable reduction in integration time or in the required sensitivity of a receiver. Other standards such as heated glass plates,<sup>1</sup> which are probably almost black in the region of interest but have not been rigorously demonstrated to be so, can also be calibrated. However, the advantages of using a glass plate over a cavity are slight, therefore, a mercury lamp is the only secondary standard considered in this report.

If additional measurements are made of the transmission characteristics of the spectrometer, the standard source can then be used to calibrate responsivity of detectors. This was done for the detector used in these measurements; some results will be presented in a later section. Complete determination of the transmission characteristics of a monochromator is involved and will not be presented here in entirety.

### THEORY OF THE BLACKBODY CAVITIES

The two types of cavities considered are an open cone and a partially closed cylinder, with the internal cross sections shown in Fig. 1. The surface is smooth cast iron, blackened with carbon soot, and is considered to have reflection properties intermediate between diffuse and specular. For diffuse reflection, we can use the method of Gouffe<sup>7</sup> in which the fraction of the energy emerging at each reflection is essentially  $\rho s/S$  where  $\rho$  is the surface reflectivity and  $s/S$  is the ratio of opening to cavity surface. After  $n$  reflections, the total emerging energy for unit input is

$$\rho_o = \rho s/S [1 + \rho(1 - s/S) + \rho^2(1 - s/S)^2 \dots + \rho^n(1 - s/S)^n].$$

Assuming  $n$  large, summing, and substituting  $\epsilon = 1 - \rho$ , we obtain an emissivity  $\epsilon_o = 1 - \rho_o$  for the opening

$$\epsilon_o = 1/[1 - s/S + s/\epsilon S]. \quad (1)$$

Although the assumption that  $\rho s/S$  is the fraction of the energy re-emitted at each reflection is only exact for a sphere, Gouffe has shown that the result is not significantly different for other geometries.

In the other extreme, for specular reflection we assume probabilistically that the number of reflections of a ray between entry and emergence is  $n = 0[S/s]$ . For a cone we can show that this value of  $n$  is correct within a small factor. From the ray given in Fig. 1 it is seen that  $\theta_n = \phi + 2n\theta$  where  $n$  is the number of reflections. The ray reverses at  $\theta_n = \pi/2$  and thus for  $\phi$  and  $\theta$  small,<sup>8</sup>  $n \approx \pi/2\theta$ , which we can show from the geometry is equivalent to

$$n \approx S/s. \quad (2)$$

By a repeated application of the reflection formula, the emissivity of a cone with specular reflection would therefore be given by

$$\epsilon_0 = 1 - (1 - \epsilon)^{S/s}. \quad (3)$$

For a wide range of configurations and material emissivities, Eq. 3 gives  $\epsilon_0 \approx 1$  and may be considered as the upper limit of the emissivity for our investigations.

From the dimensions of Fig. 1, we take  $S/s = 18$  (cone) and  $S/s = 160$  (cylinder). For this wide disparity in surface ratios, if we assume that the reflection processes are at all comparable for the two cavities, the emissivities of the two cavities will be nearly equal to each other only if  $\epsilon_0 \approx 1$  for both cavities. This is the basis for transforming relative to absolute measurements. If we consider the two limiting cases (Eqs. 1 and 3) and calculate  $\epsilon_0$  for each cavity as a function of  $\epsilon$ , we obtain the results of Table I. Comparing columns 1 and 3, or 2 and 4, we find that for either case, if  $\Delta\epsilon_0/\epsilon_0$  (cylinder)  $\leq .25$ , then

$\epsilon_0$  (cylinder)  $> .95$ , i. e., if the difference in the emissivities is not greater than 25%, the emissivity of the cylindrical cavity differs from unity by less than 5%.

For the two limiting cases the surface emissivities,  $\epsilon$ , are greatly different for a given  $\Delta\epsilon_0/\epsilon_0$ . The intermediate case of partial reflection has been treated by de Vos<sup>9</sup> but is difficult to apply to our geometry. However, since we are interested only in insuring that, for a given  $\Delta\epsilon_0$ ,  $\epsilon_0$  is near unity, only the limiting cases need be considered. Direct measurements of  $\epsilon$  have been made which indicate that the reflectivity is intermediate between specular and diffuse, but more closely to approximating specular reflection. By assuming the worst case ( $\epsilon_0$  smallest for a given  $\Delta\epsilon_0$ ) of diffuse reflection we have a lower bound on  $\epsilon_0$ .

#### BLACKBODY CAVITY DESIGN AND SECONDARY STANDARD

A cross sectional view of the conical blackbody is shown in Fig. 2. Two heating elements, individually controlled with automatic thermostats, maintained the temperature of the iron at  $480^\circ \text{K} \pm 10^\circ$ . An external thermostat was used to check the temperature within the cavity. The insulation was designed such that the major heat loss was by radiation through the opening. The outside stainless steel jacket remained essentially at room temperature. Because the spectrometer accepted a narrow solid angle of incident radiation (as discussed in the next section), the radiation accepted by the spectrometer came almost completely from the opening to the blackbody.



The secondary standard was a commercial mercury arc lamp (General Electric UA-2) operated at 92 volts with the GE transformer (9T65Y14) and dropping resistor of 20 k $\Omega$  in series with the starter. The lamp was not cooled or shielded. Although the lamp geometry was not identical with the blackbody aperture, the useful areas can be compared and the factor included in the calculation of equivalent blackbody temperature of the lamp. The useful area of the lamp was approximately the same as the area of the blackbody apertures.

### EXPERIMENTAL ARRANGEMENT

A schematic diagram of the spectrometer is shown in Fig. 3. A tapered light-pipe transmits the radiation from the output light-pipe of the spectrometer (2-cm i. d.) to the 4-mm i. d. entrance to a small cavity containing the detector. From the relation<sup>10</sup>

$$D_1 \sin \theta_1 = D_2 \sin \theta_2, \quad (5)$$

where  $D_1$  is the diameter of the exit light-pipe,  $D_2$  the diameter of the detector opening, and  $\theta_1$  and  $\theta_2$  are the angles an outermost ray can make with the axis, we can obtain the maximum angular divergence accepted by the spectrometer. Setting  $\theta_2 = \pi/2$  (maximum angle to enter detector cavity) we obtain  $\sin \theta_1 = 1/5$  or  $\theta_1 = 11.5^\circ$ . The entrance and exit light-pipes of the cavity are optically nearly symmetrical, giving an acceptance F-number of F-2.5. The actual F-number, which was maintained through the spectrometer, was approximately F-3. Within the acceptance cone of the spectrometer, virtually all of the radiation leaving the blackbody source is accepted by the detector.

The detector used for the experiments is an InSb photodetector operated at pumped liquid-helium temperatures in a strong magnetic field. The detector has been described by Putley,<sup>6</sup> and the particular detector used in these experiments was manufactured by Advanced Kinetics. To use a blackbody as a primary standard for calibrating either secondary standards or the spectrometer-detector system, it is necessary to know the linearity of the system. Both bolometers and photodetectors are ideally square-law devices, i. e., linear in the sense that the voltage output is linearly proportional to the power input. To test this proportionality over as wide a range as possible, a diaphragm was placed between spherical mirrors 1 and 2 with a variable aperture. The known decrease in the incident power with decreased aperture can be compared with the decrease in voltage at the detector output. The linearity of the detector was verified within the range necessary to calibrate the secondary standard.

To determine the responsivity (volts/watt) of the detector as a function of frequency, it is necessary to obtain the transmission characteristics of the spectrometer. The study of these characteristics is involved and will be presented elsewhere. Transmission characteristics,  $T_m(\nu)$ , of the complete optical system, can be evaluated approximately. In terms of this transmission characteristic, the output voltage from the detector is given by

$$V_{\text{out}} = R_d(\nu)T_m(\nu)P_{\text{BB}}(\nu), \quad (6)$$

where  $R_d$  is the responsivity of the detector and  $P_{\text{BB}}$  is the blackbody

power. Having measured  $V_{\text{out}}$  and  $T_m$ , and having calculated  $P_{\text{BB}}$   $R_d$  is directly determined from Eq. 6.

A block diagram of the complete system is shown in Fig. 4. The entrance light-pipe of the spectrometer can be switched between identical inputs, so that a high-level pulsed signal can be compared with low-level signals from the radiometer and blackbody. The output of the detector can be manually connected either to a scope or to the lock-in amplifier, depending on the input. Mechanical filtering is required as the detector is piezo-electric. Measurements with the mercury arc source required a 3-sec electrical integration time with additional accuracy obtained by recording the output for approximately 2 min and averaging. Measurements with the blackbody cavities required electrical integration with a 10-sec time constant and an additional recorder integration of 10 min. The minimum detectable signal at the output of the detector was approximately  $10^{-9}$  V. This corresponded to a minimum detectable blackbody power at the long wavelength end of the spectrum of approximately  $2 \cdot 10^{-10}$  W/sr at a wavelength of 2 mm (2000  $\mu$ ). The short wavelength limit was determined by the cutoff of the detector.

## EXPERIMENTAL RESULTS

In Fig. 5 the raw data of detector output in nanovolts ( $10^{-9}$  V) is given for the two blackbodies and for the mercury arc lamp. The discontinuities in the output voltage are due to the variation in the spectrometer transmissivity at a given frequency with different gratings. We consider first the relative emissivities of the two blackbodies,  $\Delta\epsilon/\epsilon_0$ .

In Fig. 6 we plot the reflectivity of the soot-coated, cast iron surface. This was obtained by comparing the reflectivity of a soot-coated, cast iron mirror with an aluminium mirror, assuming  $\rho = 1$  for the aluminium. Using the values of  $\Delta\epsilon_0/\epsilon_0$  and  $\epsilon$  from Figs. 5 and 6, we find that by comparing with the data from Table I, the reflection is intermediate between diffuse and specular. However, despite the large variations in  $\Delta\epsilon_0/\epsilon_0$  and  $\epsilon$ ,  $\epsilon_0$  for the cylinder is almost unity throughout the frequency range.

For the lowest frequencies ( $\lambda > 1$  mm) the conical cavity differed considerably from a blackbody, and a better blackbody comparison was necessary. In constructing a third cavity, a flint glass cone replaced the metal cone. The reflectivity of the glass is plotted in Fig. 6, where it can be seen that the glass cone should very closely approximate a blackbody. (A 1/8-in. glass plate was found to transmit only 2.5% of the incident energy.<sup>11</sup>) The long wavelength radiation from the conical glass cavity and the cylindrical cavity were almost identical, thus verifying the contention that the cylindrical cavity is very close to a blackbody.

Assuming that the cylindrical cavity is a blackbody at  $483^\circ$  K, we can calculate the equivalent blackbody temperature of the mercury arc lamp by comparing the relative responses, provided the detector is linear. In Fig. 7 the detector output is plotted versus the diameter of an aperture under parallel illumination. Except at the largest diameter, where the illumination is not expected to be uniform, the output is directly proportional to area, verifying the linearity of the detector.

In Fig. 8 the equivalent blackbody temperature of the lamp is given as a function of frequency. The points represent an average of two to four measurements with the error bars indicating the rms deviation. The points without error bars represent single measurements. The variability of the computed temperature comes mainly from two sources, slow variations of the lamp intensity with time and drift of the zero level of the lock-in amplifier. The first source of variability represents a true change of temperature and must be accounted for when using a mercury arc lamp as a secondary standard. The second source of variability arises in the low level blackbody measurements and thus results in a spurious temperature variation of the arc lamp when the intensities are compared. The two sources of variability can be comparable in magnitude. A third source of variability can arise from changes in the detector sensitivity. Although this source of measurement error can be very serious, it was possible to reduce the error to a relatively small value by operating under carefully controlled conditions. Although the relative values of the equivalent arc lamp temperature should be valid to within the error bars for most points, the entire temperature may be as much as 20% low. This arises from the calculation of the equivalent area of the lamp which we took to be equal to the blackbody area but may be somewhat smaller.

It should be noted here that the results embodied in Fig. 5 are sufficient to obtain absolute radiated power of an unknown signal. Assuming  $\epsilon_0 \approx 1$  for the cylindrical cavity, we can calculate the volts/watt for the monochromator-detector system from Fig. 5 and the known

blackbody emission. In fact, our system is constructed so that a calibration can be obtained almost simultaneously with pulsed radiation measurements. The same procedure can also be utilized with shorter integration times by employing the secondary standard.

It is interesting, for its own sake, to calculate the responsivity of the detector. In Fig. 9 we plot the detector responsivity (volts/watt) from the results obtained by using the secondary standard (mercury arc lamp) and the calculated blackbody radiation determined from its equivalent temperature.<sup>12</sup> A frequency bandwidth of  $\Delta f/f = 0.1$ , taken for the in-blaze grating angle, was calculated and checked experimentally. The source was determined to have  $4 \text{ cm}^2$  area with a solid angle of 0.1 radian. The total in-blaze attenuation of the monochromator was measured to be 13 dB. Using this value of attenuation for  $T_m$ , substituting for the blackbody power from the above data, and the detector output from Fig. 5, we calculate the detector responsivity from Eq. 6 as given by the dashed curves. The effects of the main grating, filter gratings, diffraction and shadowing effects can be included, considerably smoothing the response. However, for the purposes of this study, it is sufficient to connect the response peaks which coincided most closely with the parameters chosen for the calculation. The solid line represents the detector responsivity determined in this manner. The single point at 4-mm wavelength was measured with a 4-mm klystron oscillator.

This particular responsivity characteristic corresponded to a magnetic bias field of 12 kG and a bias current of 90  $\mu\text{A}$  which were found to give optimum response both for 4-mm wavelength and for radiation integrated over the entire blackbody spectrum. The operating

temperature of the detector was  $2^{\circ}$  K. The results differ markedly from the original results of Putley<sup>6</sup> but agree substantially with his later results.<sup>13</sup>

The same method can be used to calibrate other detectors with comparable responsivities. Using the secondary standard, lower responsivity detectors can also be calibrated.

#### ACKNOWLEDGMENTS

This work was supported in part by the Joint Services Electronics Program (U. S. Army, U. S. Navy, and U. S. Air Force) under Grant No. AF-AFOSR-139-64; the U. S. Air Force under Contract No. AF33(615)-1078, and the National Science Foundation under Grant No. NSF GP-2239.

#### FOOTNOTES

1. G. N. Harding, et al., Proc. Phys. Soc. 77, 1069 (1961).
2. A. J. Lichtenberg, S. Sesnic, and A. W. Trivelpiece, Phys. Rev. Letters 13, 387 (1964).
3. G. B. Field, J. Geophys. Res. 64, 1169 (1959).
4. W. L. Einmann, R. L. Bates, and J. D. Merriam, J. Opt. Soc. Am. 53, 729 (1963).
5. C. S. Williams, J. Opt. Soc. Am. 51, 564 (1961).
6. E. H. Putley, J. Phys. Chem. Solids 22, 241 (1961).
7. A. Gouffe, Rev. Opt. 24, Nos. 1-3 (1945).

8. The restriction of  $\phi$  small implies that the conical cavity is only a blackbody within a small angle of diverging rays. Since the monochromator used for the measurements only accepts a narrow cone of rays, the requirement was satisfied over the entire acceptance.
9. J. C. De Vos, *Physica* 20, 669 (1954).
10. Eq. 5 follows directly from the general principle of conservation of phase space, A. J. Lichtenberg, *Nucl. Inst. Methods* 26, 243 (1964), but can also be proved geometrically.
11. From those measurements it is also apparent that a hot glass plate can be used as a standard source, provided high accuracy is not needed.
12. For the detector responsivity given in Fig. 9 is the radiation taken to be that entering the LHe Dewar light pipe; thus the attenuation in the light pipe, and the loss in power due to reflection at the InSb crystal and absorption in the windows, are included in the overall responsivity. In contrast, the responsivity reported by Putley does not include these losses. The actual responsivity of the InSb, itself, is at least a factor of 2 larger if these losses are included. However, it has not been possible to determine the losses exactly.
13. E. H. Putley and N. Shaw, R.R.E. Memo 2115, August 1964.



TABLE I

Comparison of emissivities for conical and cylindrical cavities

$\epsilon$ / $\epsilon_0$	cone		cylinder	
	diffuse reflection $\frac{1}{1 + 1/18\epsilon}$	specular reflection $1 - (1 - \epsilon)^{18}$	diffuse reflection $\frac{1}{1 + 1/160\epsilon}$	specular reflection $1 - (1 - \epsilon)^{160}$
.2	.78	-	.97	-
.1	.645	-	.94	-
.05	.475	.985	.875	1.000
.025	-	.87	-	1.000
.01	-	.55	-	1.000

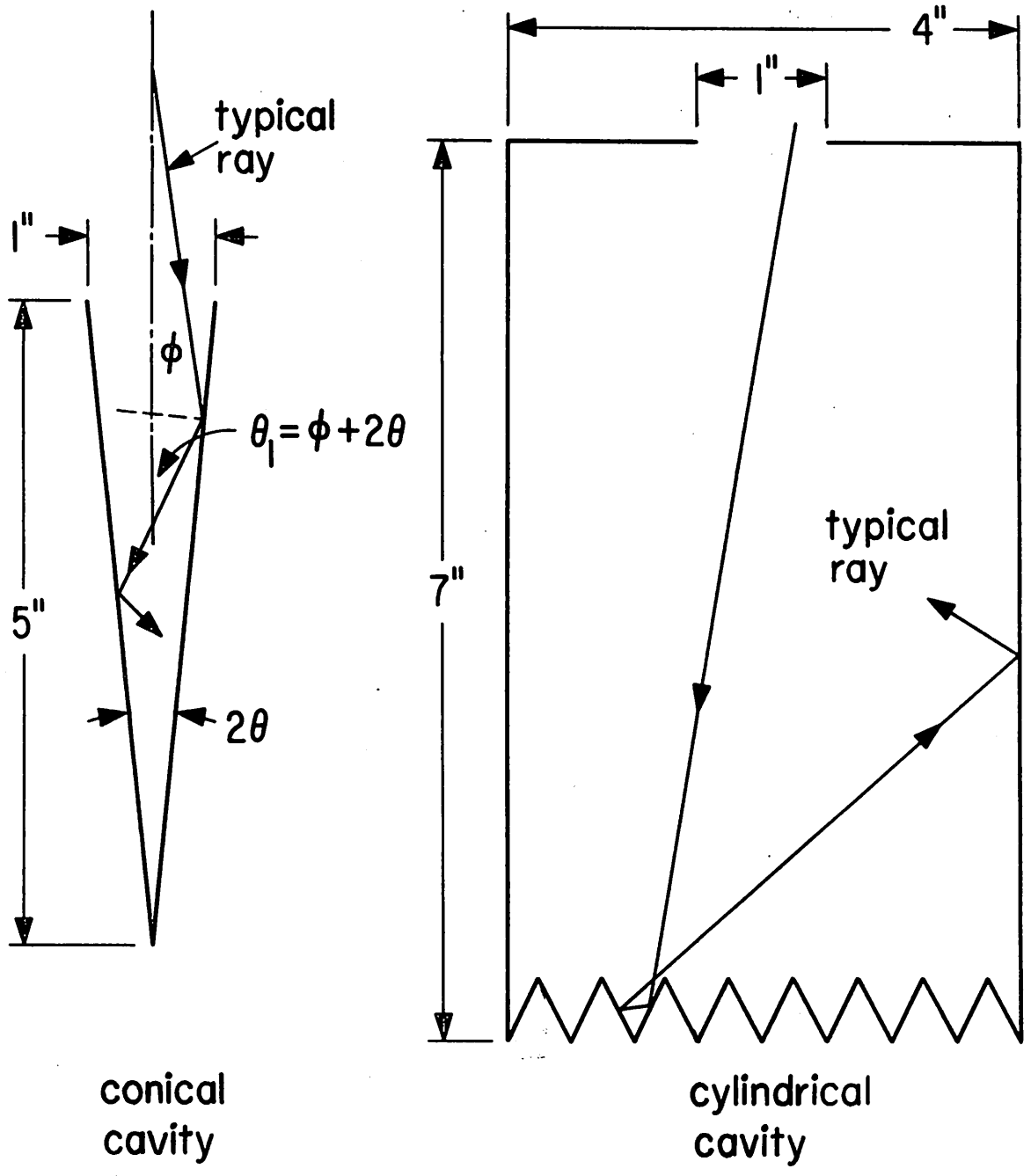


Fig. 1. Internal cross sections of blackbodies.

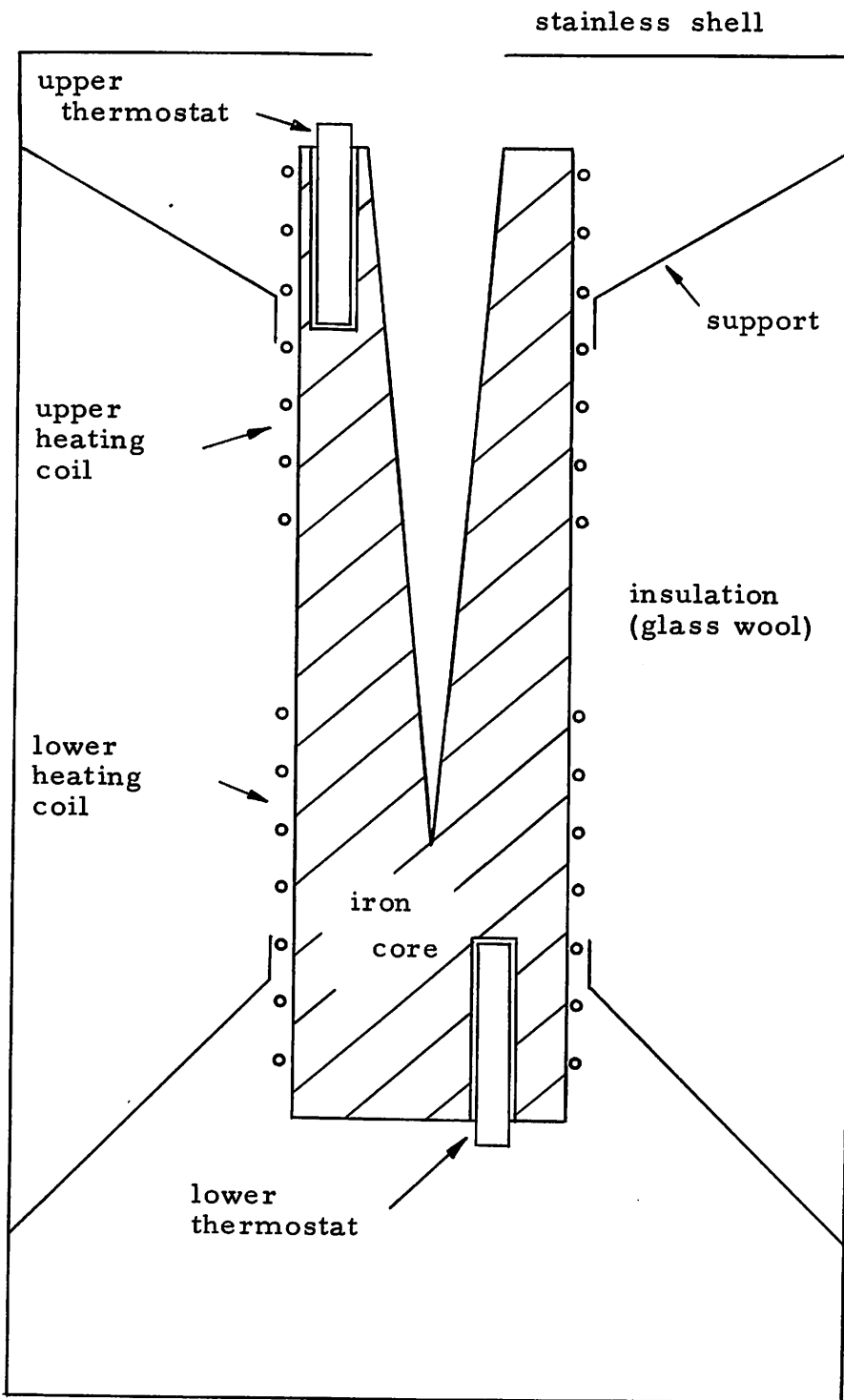


Fig. 2. Cross section of complete conical blackbody.

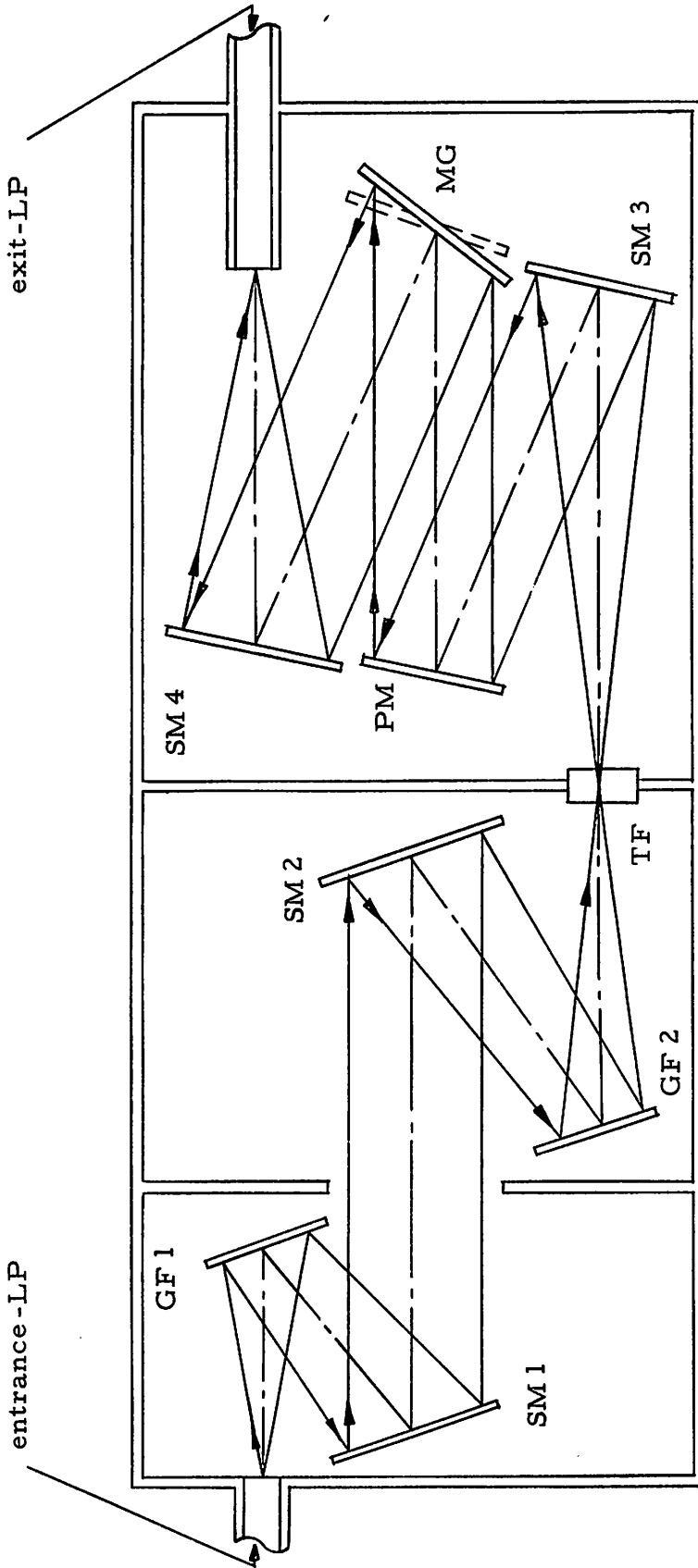


Fig. 3. Schematic diagram of the spectrometer. MG-Main Grating, GF-Grating Filter, SM-Spherical Mirror, PM-Plane Mirror, TF-Transmitter Filter, LP-Light Pipe.

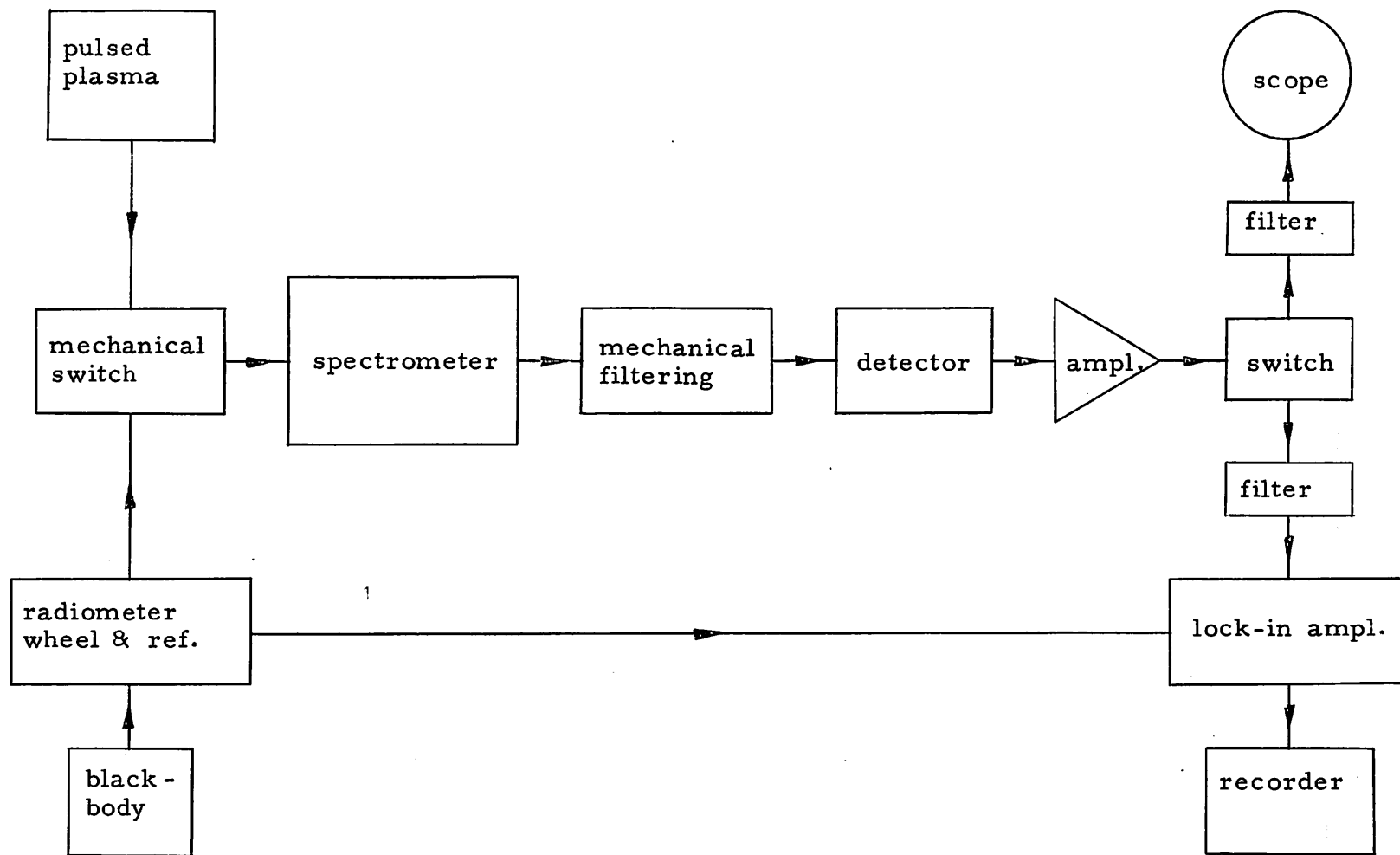


Fig. 4. Block diagram of complete system.

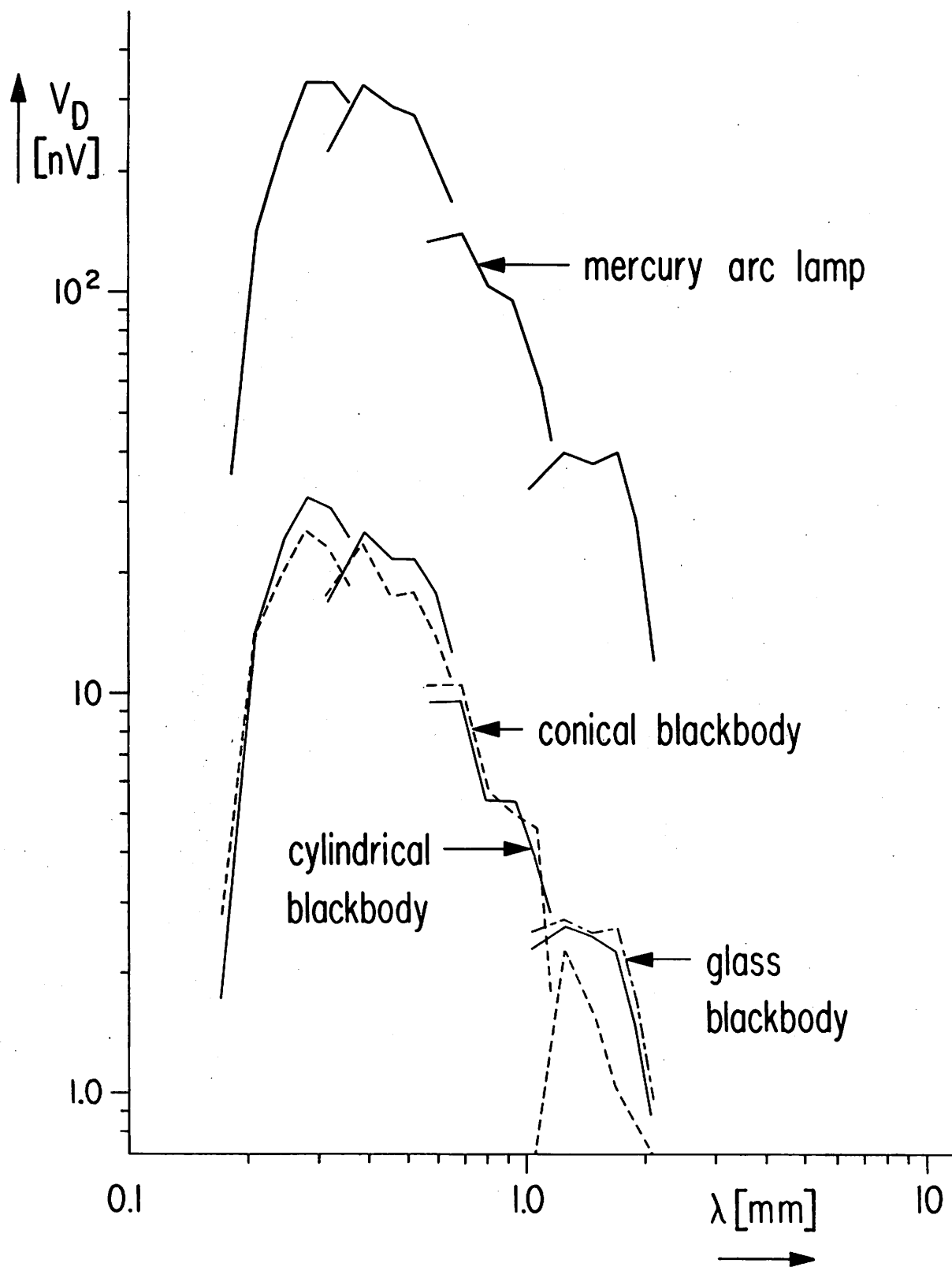


Fig. 5. Detector output voltage for blackbodies and mercury discharge.

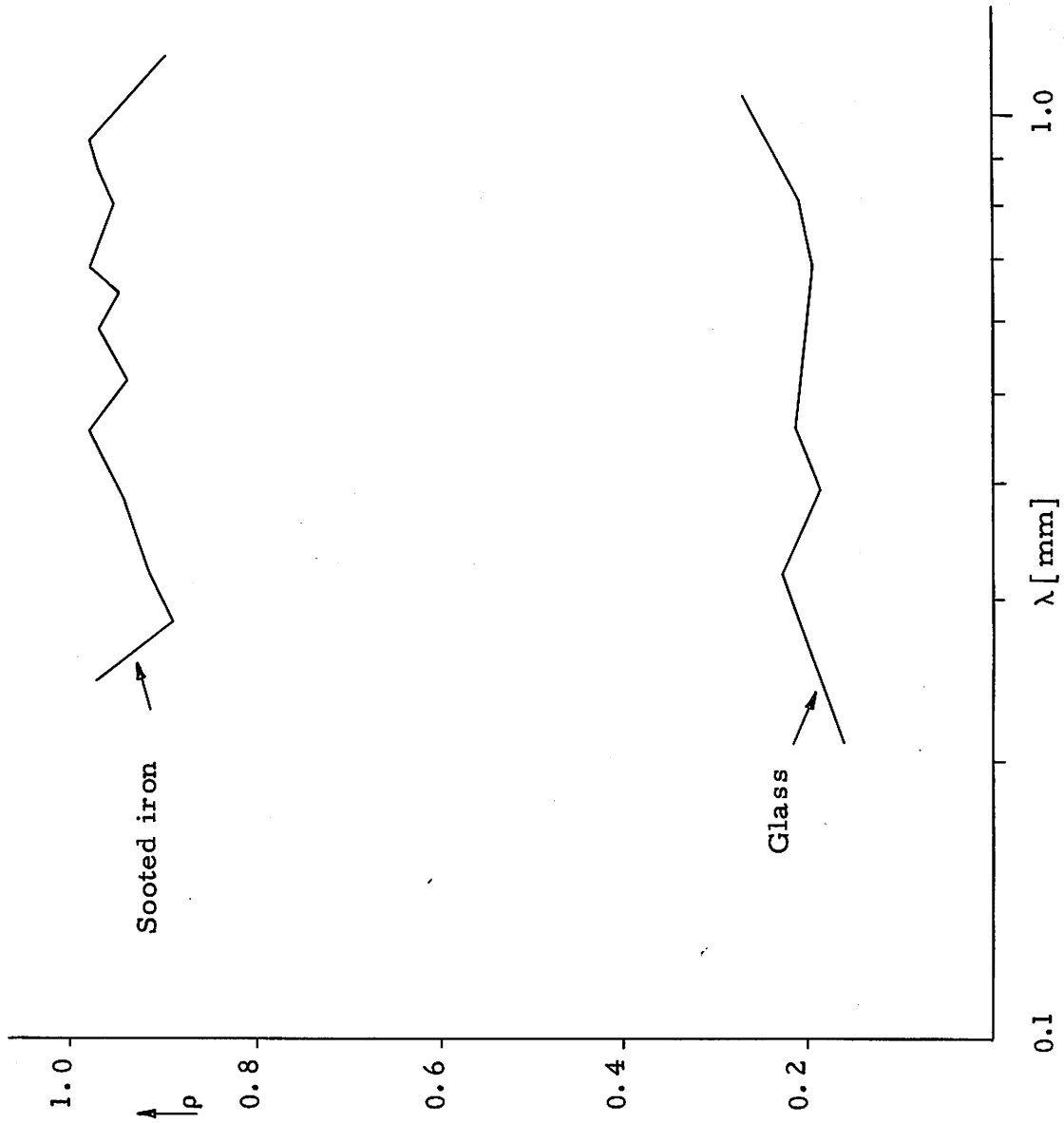


Fig. 6. Reflectivity of soot-coated cast iron and flint glass.

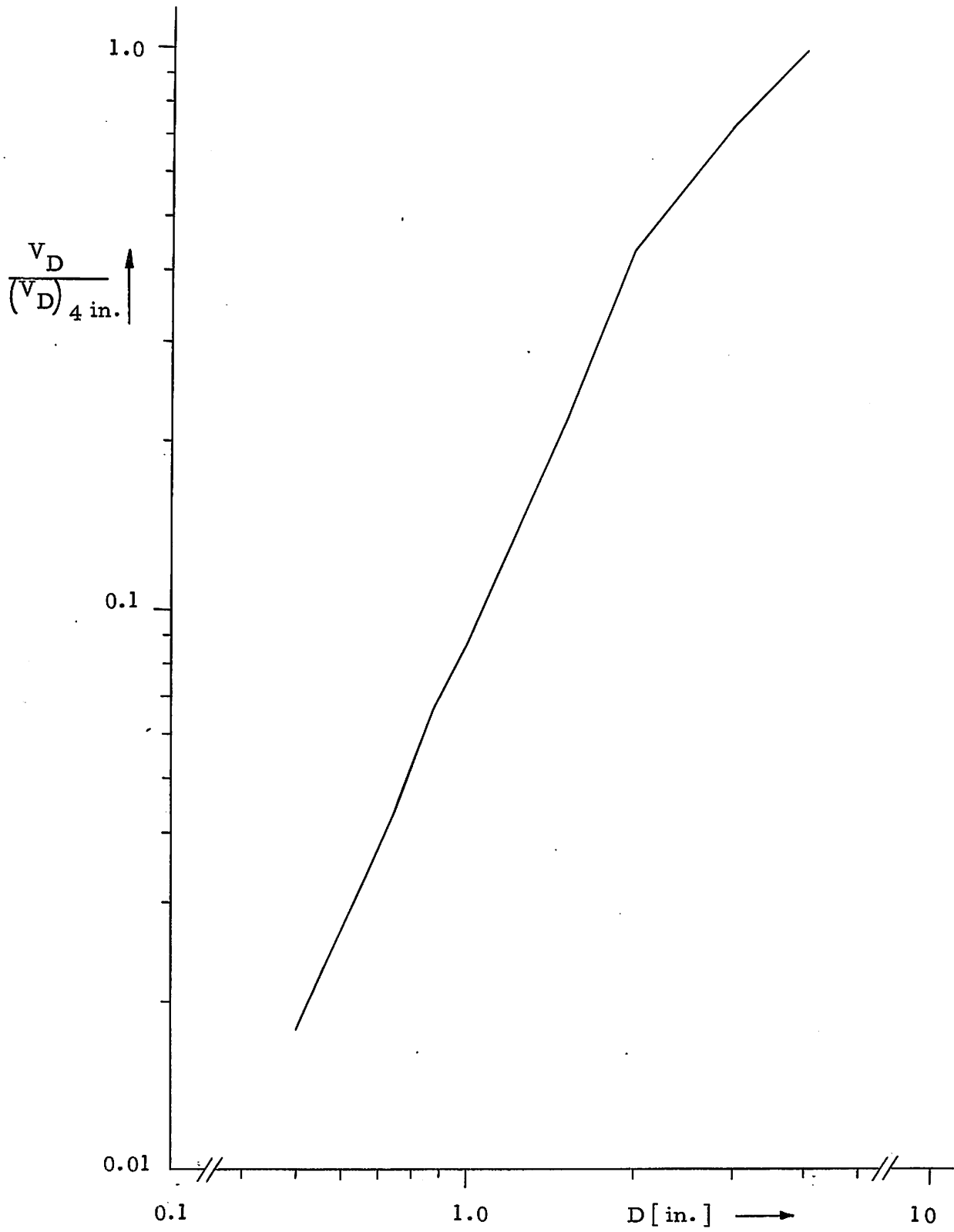


Fig. 7. Variation of detector output with aperature.



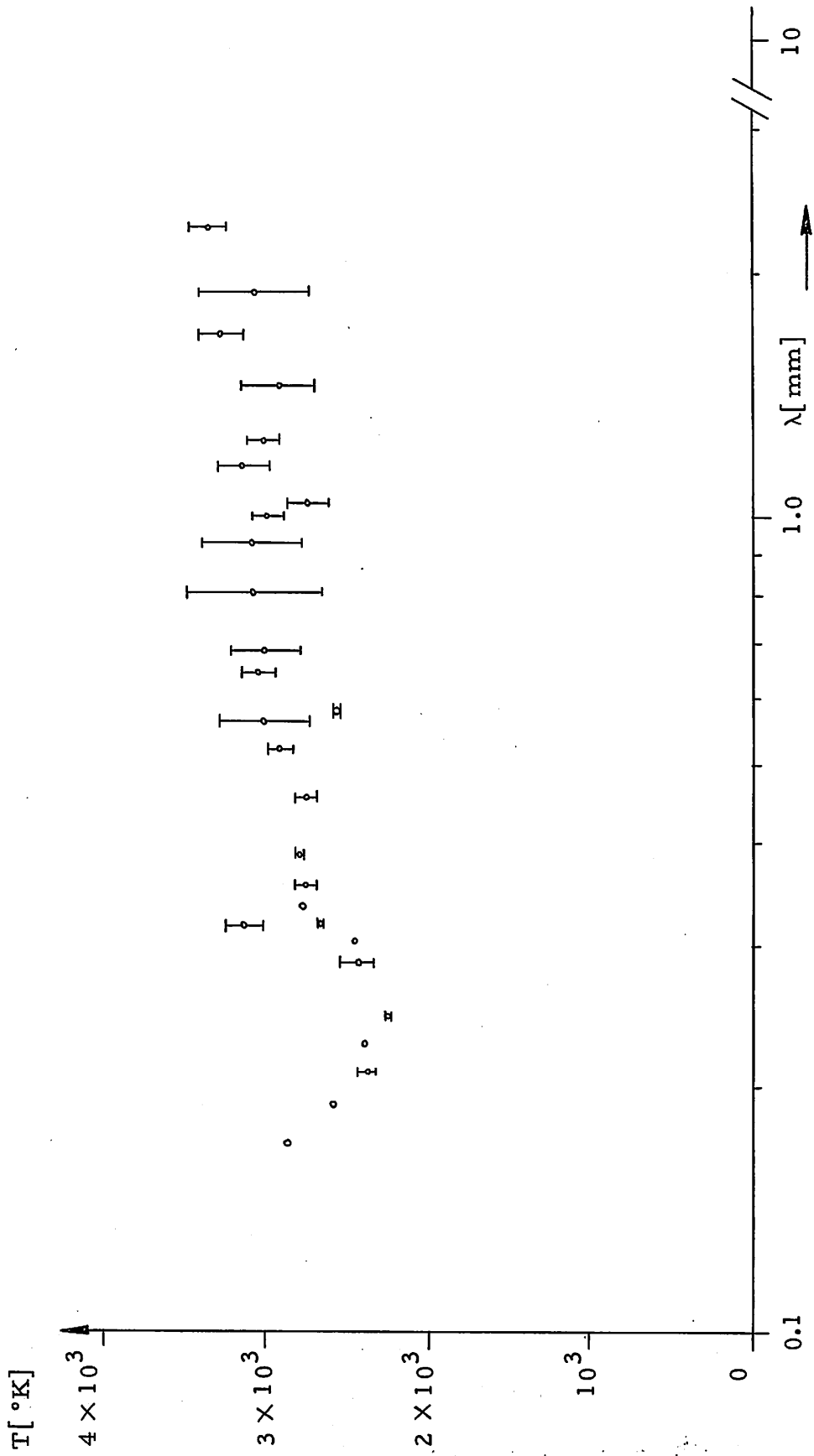


Fig. 8. Equivalent blackbody temperature of mercury lamp as a function of frequency.

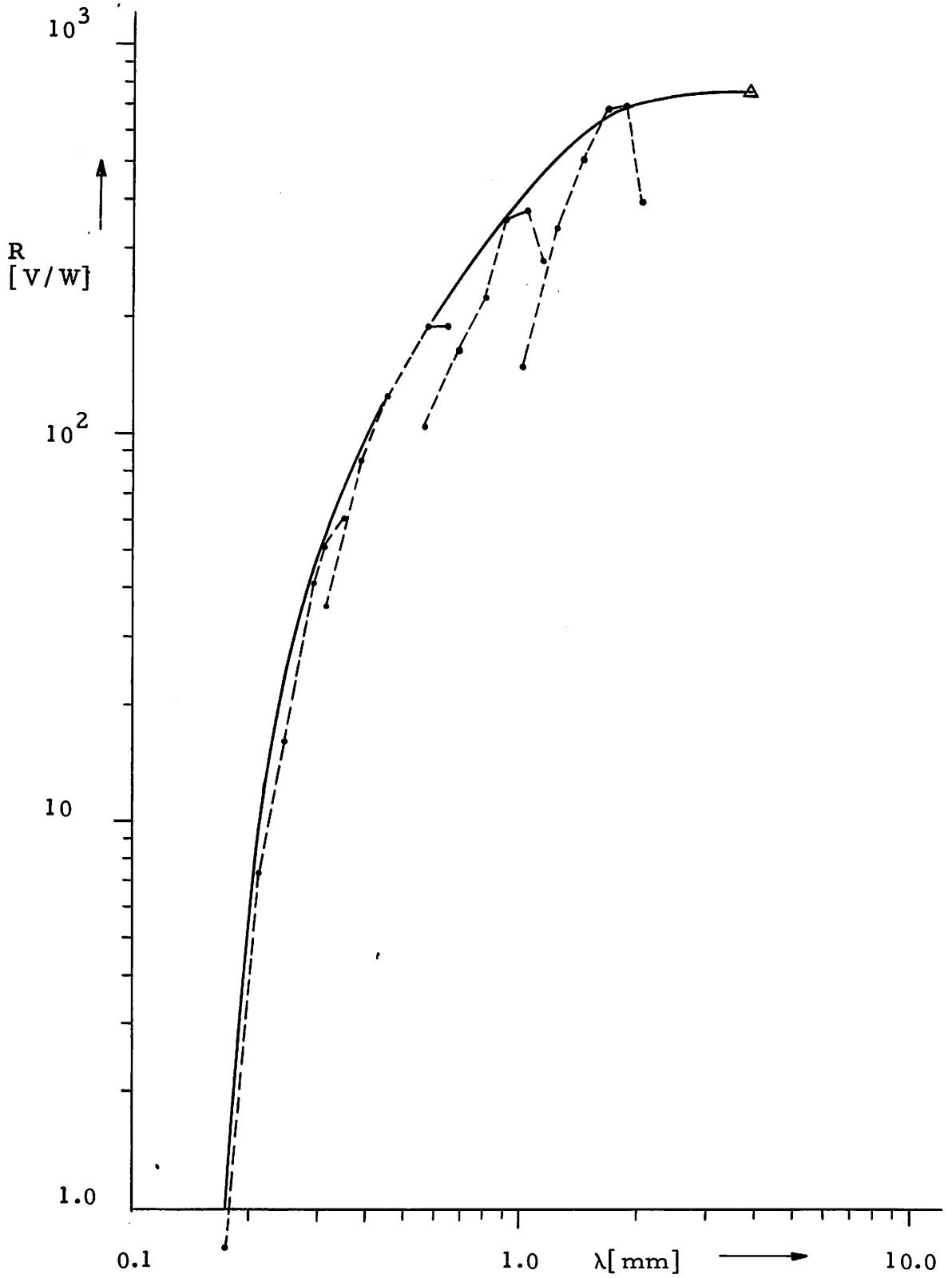


Fig. 9. Responsivity volts/watts of InSb detector  $T = 2^\circ\text{K}$ ,  
 $I_{\text{bias}} = 90 \mu\text{a}$ ,  $B = 12 \text{kG}$ .